

Insulating boundary layer and magnetic scattering in $\text{YBa}_2\text{Cu}_3\text{O}_{7-\delta}/\text{Ag}$ interfaces over a contact resistivity range of 10^{-8} – $10^{-3} \Omega \text{ cm}^2$

S. C. Sanders, S. E. Russek, C. C. Clickner, and J. W. Ekin
*Electromagnetic Technology Division, National Institute of Standards and Technology,
Boulder, Colorado 80303*

(Received 11 May 1994; accepted for publication 16 August 1994)

We have measured interface transport in thin-film $\text{YBa}_2\text{Cu}_3\text{O}_{7-\delta}/\text{Ag}$ interfaces having resistivities ranging from 10^{-8} to $10^{-3} \Omega \text{ cm}^2$. Analysis of the interface I - V data indicates that tunneling is the predominant transport mechanism even for the *in situ* interfaces having contact resistivities of 1 – $7 \times 10^{-8} \Omega \text{ cm}^2$. Zero-bias conductance peaks are also observed for the entire range of interface resistivity. The similarity of the zero-bias conductance peaks among these widely varying interfaces suggests that the low-temperature interface transport is governed by the same mechanism in each case. These conductance peaks are analyzed in the framework of the Appelbaum–Anderson model for tunneling assisted by magnetic scattering from isolated magnetic spins in the interface. © 1994 American Institute of Physics.

We report interface transport results for planar, c -axis-oriented $\text{YBa}_2\text{Cu}_3\text{O}_{7-\delta}$ (YBCO)/normal-metal interfaces in which the interface resistivities vary from 10^{-8} to $10^{-3} \Omega \text{ cm}^2$. This wide range of resistivities was obtained by systematically exposing the YBCO films to various surface treatments, such as subjecting to air, N_2 , or CO_2 , or etching with Br-methanol or an Ar-ion beam, prior to depositing an Ag overlayer. *In situ* interfaces (in which the Ag overlayer was deposited immediately after fabricating the YBCO film and without breaking vacuum) gave the lowest contact resistivity,¹ while *ex situ* interfaces² formed after ion etching the YBCO surface gave the largest contact resistivity. The central result of this letter is that tunneling through an insulating layer between the YBCO and Ag appears to be the dominant interface transport mechanism, at low temperatures, even for the *in situ* interfaces. Moreover, zero-bias conductance peaks having similar character are observed over the entire range of interface resistivities. These conductance peaks suggest that magnetic scattering contributes significantly to the interface transport in these samples. Although we have not yet identified the particular magnetic scatterers, the similar peak characteristics over the large range of contact resistivities suggest that the magnetic scatterers giving rise to the peaks are present at the “intrinsic” degraded YBCO surface.

Understanding, predicting, and controlling electrical transport at thin-film YBCO/normal-metal interfaces is required for advances in superconductive devices based on proximity or Josephson effects, as well as superconducting microcircuit transmission line applications. Many groups have fabricated SN and SNS devices based on high- T_c superconductors, and progress has been steady.^{3–7} For applications that use a large number (up to thousands) of junctions or contact interfaces on a single chip, however, uniformity and reproducibility of junction critical currents and resistivities are crucial requirements which have yet to be adequately obtained, and the interface resistivity often dominates the device resistivity. A deeper understanding of the transport mechanisms across YBCO/normal-metal interfaces is required to control or minimize interface resistivity.

There are a number of papers on interface transport and tunneling measurements between high- T_c superconductors and normal metals in the literature. Many report zero-bias peaks in the conductance versus voltage (G - V) characteristics, often called zero-bias anomalies (ZBAs). Recent papers^{8–10} have reported more detailed studies of ZBAs, and several explanations for the origin of ZBAs in YBCO/normal-metal interfaces have been offered. The most frequently invoked explanation for conductance ZBAs is that of tunneling assisted by scattering from isolated (noninteracting) magnetic impurities (spins) in the interface. This was originally modeled for metal-insulator-metal junctions by Appelbaum¹¹ and Anderson.¹² Most of the samples in the ZBA studies reported to date have had large interface resistances due to “natural barriers” formed by air exposure before counterelectrode deposition, and often the geometry of the contact areas was not well defined. These sample characteristics limit to some degree the information that can be obtained from these transport experiments, the origin of the isolated magnetic spins being an example.

For this study, YBCO films 200 nm thick were fabricated on polished (100) MgO or (100) LaAlO_3 substrates by pulsed laser deposition.² The chamber base pressure with the substrate at deposition temperature was $\sim 10^{-5}$ – 10^{-4} Pa ($\sim 10^{-7}$ – 10^{-6} Torr). Following YBCO deposition, films were cooled to room temperature in an oxygen ambient of 26.7 kPa (200 Torr). The resulting c -axis-oriented films [which had full width at half-maximum (FWHM) $< 0.5^\circ$ for the 005 rocking curves] had T_c 's ranging from 86–91 K and J_c 's of ~ 3 – 5×10^6 A/cm² at $T = 77$ K. Scanning tunneling microscopy data taken on separate films prepared under identical conditions show spiral growth for YBCO on MgO and island growth for YBCO on LaAlO_3 , with the area of the YBCO a - b edges about 5% of the c -axis area.¹³ After cool down, the YBCO films were either coated immediately with a 200 nm overlayer of evaporated Ag (to study interfaces formed *in situ*)¹ or subjected to a selected surface treatment.² The YBCO surface treatments included air, CO_2 , or N_2 exposures, or Br-methanol or Ar-ion etches. The Br-methanol and 200 V Ar-ion etches were calibrated to remove the top

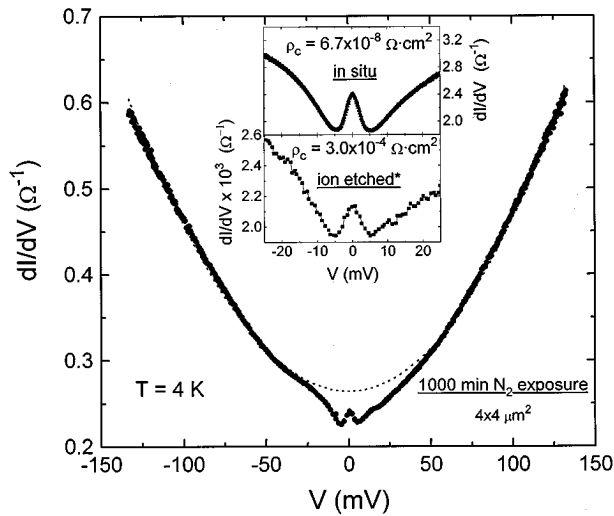


FIG. 1. G - V for a planar, c -axis YBCO/Ag interface formed after exposing the YBCO surface to N_2 gas for 1000 min at room temperature. Inset: Low-bias data indicating the similarity of the zero-bias peaks for YBCO/Ag interfaces having nearly four orders of magnitude difference in their resistivities. The top data set is for a $4 \mu\text{m} \times 4 \mu\text{m}$ *in situ* interface, and the bottom data set is for an $8 \mu\text{m} \times 8 \mu\text{m}$ *ex situ* interface.

1–3 nm of YBCO. Following the Ag overlayer evaporation, the samples were photolithographically patterned to define planar interfaces (square contact areas having 2, 4, 8, and 16 μm sides) between the YBCO and the Ag overlayer. A 500-nm-thick Ag top electrode was used to contact the devices. Conductance curves were obtained by differentiating the I - V data using a sliding three-point fit.

Several features of the conductance data for the YBCO/Ag interfaces indicate that tunneling is the dominant transport mechanism at low temperatures. Figure 1 shows G - V data for a YBCO/Ag interface in which the YBCO film was exposed to N_2 gas prior to Ag deposition. A nearly parabolic background at high biases is clearly evident. Parabolic conductance backgrounds are indicative of tunneling in the normal state,¹⁴ and are observed in all of our samples where backgrounds are measurable. (Sufficient contact resistance is needed to reach the required bias voltages before exceeding the critical current of the superconducting material adjacent to the interface.) The conductance deviates negatively from parabolic behavior near 20 mV. This has been attributed in the past to a gaplike feature.^{8,9} Perhaps the most conspicuous feature of the data reported here is the zero-bias peak in the G - V curves. These peaks were observed for nearly all of the YBCO/Ag interfaces measured, including *in situ* interfaces having $T=4$ K contact resistivity $\rho_c \sim 10^{-8} \Omega \text{ cm}^2$. The inset of Fig. 1 compares G - V for an interface formed *in situ* with a YBCO/Ag interface formed after the YBCO surface was exposed to air for 110 days, photolithographically processed, and then etched with 200 V Ar ions for 6 min. The peak shapes are similar in the two cases even though ρ_c differs by nearly four orders of magnitude. Throughout the range of interfaces studied, the character of these zero-bias conductance peaks remained similar: the peaks were typically 3–5

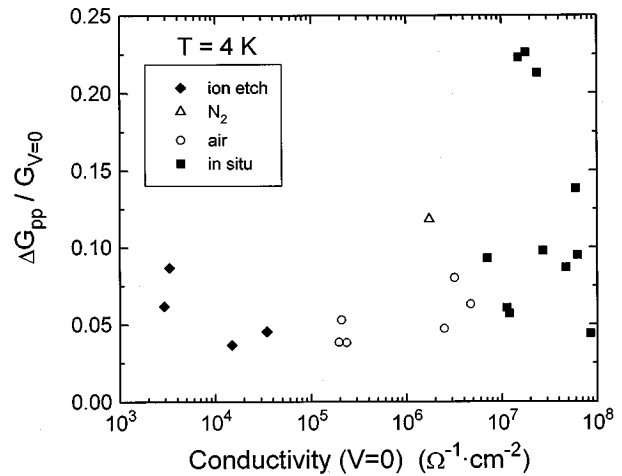


FIG. 2. Summary plot illustrating the character of the normalized peak-to-peak zero-bias conductance for planar YBCO/Ag interfaces.

mV wide and had normalized peak-to-peak heights ($\Delta G_{pp}/G_0$) of 4%–22%, as shown in Fig. 2.

Whereas we observe zero-bias conductance peaks in our c -axis YBCO/Ag interfaces, Lesueur *et al.*⁹ observed such peaks only in (100) or (103) YBCO/Pb interfaces, with c -axis YBCO/Pb interfaces producing zero-bias dips. The discrepancy might be due to the fact that our nominally c -axis samples could have a more significant conductance contribution from the a - b edges, which constitute about 5% of the total interface area in our samples having spiral or island growth morphology.¹³ Also in the case of the YBCO/barrier/Pb samples, it is likely that any exposed a - b edges are oxygen reduced at a relatively rapid rate due to the proximity of the Pb, which would diminish the conductance from the a - b edges. This is in contrast to our situation, in which the counterelectrode is a noble metal with low oxygen affinity.

The three features illustrated in Fig. 1, the parabolic background, gaplike feature, and ZBA, indicate that interface transport is occurring by tunneling. The contact resistivity results reported in Ref. 2 also contain evidence for tunneling for these interfaces. An exponential dependence of the contact resistivity on air exposure time² translates into an exponential dependence of the effective (tunnel) barrier layer thickness.¹⁵ A relatively weak temperature dependence below T_c was also observed.² Taken together, these features provide strong evidence for tunneling as the dominant low temperature interface transport mechanism in these samples, although conduction through microchannels¹⁶ at the *in situ* interfaces has not been conclusively ruled out. None of the samples investigated thus far have shown signs of Andreev reflections,¹⁷ which are expected in the clean interface limit¹⁸ and have been observed in some point-contact tunneling studies of YBCO.^{19,20}

The ZBA can be qualitatively explained in terms of the Appelbaum model^{11,12} for magnetic scattering off isolated spins located at the interface region in a metal-insulator-metal tunnel junction. The model consists of three terms for the conductance: direct tunneling (G_1), tunneling with spin

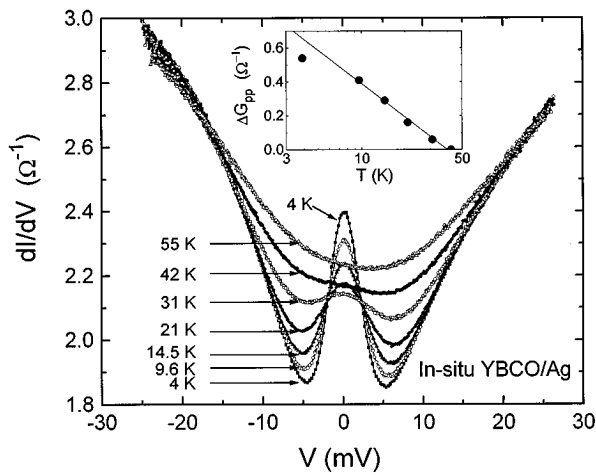


FIG. 3. Temperature dependence of the conductance of a $4 \mu\text{m} \times 4 \mu\text{m}$ *in situ* YBCO/Ag interface. The zero-bias conductance peak diminishes with increasing temperature and disappears at $T \sim 42$ K. Inset: Peak-to-peak conductance vs T on log scale for the *in situ* interface sample.

flip (G_2), and tunneling and reflection with spin flip (G_3). The latter term is responsible for the ZBA, and it has a logarithmic temperature and voltage dependence.

Figure 3 shows the temperature dependence of the conductance for an *in situ* interface. The zero-bias conductance peak diminishes as temperature is increased from 4 to 55 K. The inset indicates a logarithmic temperature dependence of the peak amplitude, consistent with the Appelbaum model. We also observe a logarithmic voltage dependence of the conductance over the range $4 \leq eV/kT \leq 10$, with thermal smearing observed at lower voltages. Figure 3 also shows that for $V > 20$ mV, the data lie on a temperature-independent background, making the gaplike feature near $V = 20$ mV more apparent.

The application of an external magnetic field perpendicular to an *in situ* interface caused a reduction in the conductance peak amplitude also, as shown in Fig. 4. The peak-to-peak conductance decreased by 30% as the field was increased from 0 to 12 T. Subtracting the zero-field conductance results in the curves shown in the upper inset. As magnetic field is increased, the zero-bias conductance decreases, but two other peaks develop on either side of the zero-bias peak. In the framework of the Appelbaum model,^{11,21} the field modifies the spin-flip tunneling G_2 due to Zeeman splitting of the impurity levels. This results in the formation of a gap, centered at zero bias, of width $2g\mu_B H$, where g is the Landé g factor of the impurity and μ_B is the Bohr magneton. The splitting of the main Kondo peak G_3 into two peaks separated by $2g\mu_B H$ was also predicted by Appelbaum. This has been observed previously in (103) YBCO/Pb junctions,⁹ where magnetic field behavior consistent with a large, field-dependent g factor was observed. In that case, the isolated magnetic spins were speculated to originate from defects at the oxygen-depleted YBCO surface. In the present study, we have not calculated a g factor, but the peak-to-peak splitting of the Kondo peak shown in the lower inset of Fig. 4 implies a large, field-dependent g factor. Our results are consistent

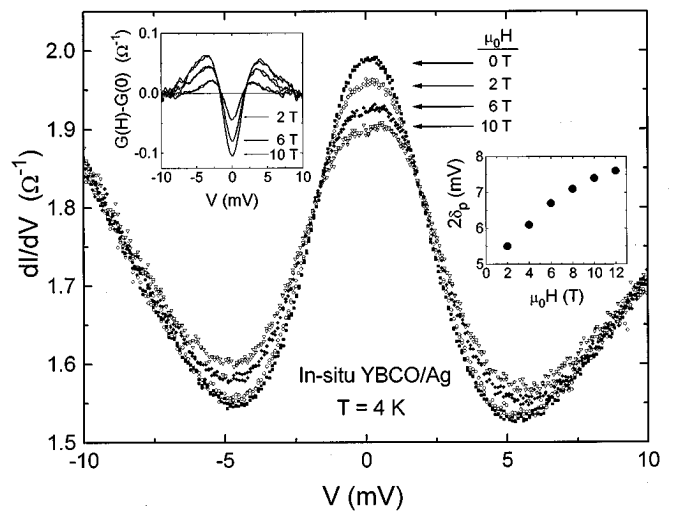


FIG. 4. Magnetic field dependence of the zero-bias conductance for an *in situ* YBCO/Ag interface. Upper inset: Subtracting the zero-field conductance reveals a splitting of the zero-bias Kondo peak and the formation of a zero-bias gap due to Zeeman splitting of the isolated magnetic spin energy levels. Lower inset: Peak-to-peak splitting of the zero-bias Kondo peak.

with the isolated magnetic spins originating at the YBCO surface, since the ZBA characteristics are independent of the barrier thickness.

This work was supported by ARPA under Contract No. 7975-01 and the NIST High- T_c program. We also acknowledge support from F. Fickett.

- ¹J. W. Ekin, S. E. Russek, C. C. Clickner, and B. Jeanneret, *Appl. Phys. Lett.* **62**, 369 (1993).
- ²S. E. Russek, S. C. Sanders, A. Rosko, and J. W. Ekin, *Appl. Phys. Lett.* **64**, 3649 (1994).
- ³N. Missert, T. E. Harvey, R. H. Ono, and C. D. Reintsema, *Appl. Phys. Lett.* **63**, 1690 (1993).
- ⁴P. A. Rosenthal, E. N. Grossman, R. H. Ono, and L. R. Vale, *Appl. Phys. Lett.* **63**, 1984 (1993).
- ⁵K. Char, L. Antognazza, and T. H. Geballe, *Appl. Phys. Lett.* **63**, 2420 (1993).
- ⁶H. Sato, H. Akoh, and S. Takada, *Appl. Phys. Lett.* **64**, 1286 (1994).
- ⁷M. I. Faley, U. Poppe, H. Soltner, C. L. Jia, M. Siegel, and K. Urban, *Appl. Phys. Lett.* **63**, 2138 (1994).
- ⁸A. M. Cucolo and R. Di Leo, *Phys. Rev. B* **47**, 2916 (1993).
- ⁹J. Lesueur, L. H. Greene, W. L. Feldmann, and A. Inam, *Physica C* **191**, 325 (1992).
- ¹⁰T. Walsh, J. Moreland, R. H. Ono, and T. S. Kalkur, *Phys. Rev. Lett.* **66**, 516 (1991); T. Walsh, *Int. J. Mod. Phys. B* **6**, 125 (1992).
- ¹¹J. Appelbaum, *Phys. Rev. Lett.* **17**, 91 (1966); *Phys. Rev.* **154**, 633 (1967).
- ¹²P. W. Anderson, *Phys. Rev. Lett.* **17**, 95 (1966).
- ¹³S. E. Russek, A. Roshko, S. C. Sanders, D. A. Rudman, J. W. Ekin, and J. Moreland, *Mater. Res. Soc. Symp. Proc.* **285**, 305 (1993).
- ¹⁴W. F. Brinkman, R. C. Dynes, and J. M. Rowell, *J. Appl. Phys.* **41**, 1915 (1970).
- ¹⁵H. Behner, K. Rührschopf, G. Wedler, and W. Rauch, *Physica C* **208**, 419 (1993).
- ¹⁶D. C. Ralph and R. A. Buhrman, *Phys. Rev. Lett.* **69**, 2118 (1992).
- ¹⁷A. F. Andreev, *Sov. Phys. JETP* **19**, 1228 (1964); **24**, 1019 (1967).
- ¹⁸G. E. Blonder, M. Tinkham, and T. M. Klapwijk, *Phys. Rev. B* **25**, 4515 (1982).
- ¹⁹N. Hass, D. Ilzyer, G. Deutscher, G. Desgardin, I. Monot, and M. Weger, *Physica C* **209**, 85 (1993).
- ²⁰V. F. Elesin, A. A. Sinchenko, A. A. Ivanov, and S. G. Galkin, *Physica C* **213**, 490 (1993).
- ²¹L. Y. L. Shen and J. M. Rowell, *Phys. Rev.* **165**, 566 (1968).